

## Inclusive Jets in PHP

---

**Philipp Roloff**<sup>\*†</sup>

CERN

*E-mail:* philipp.roloff@cern.ch

Differential inclusive-jet cross sections have been measured in photoproduction for boson virtualities  $Q^2 < 1 \text{ GeV}^2$  with the ZEUS detector at HERA using an integrated luminosity of  $300 \text{ pb}^{-1}$ . Jets were identified in the laboratory frame using the  $k_T$ , anti- $k_T$  or SIScone jet algorithms. Cross sections are presented as functions of the jet pseudorapidity,  $\eta^{\text{jet}}$ , and the jet transverse energy,  $E_T^{\text{jet}}$ . Next-to-leading-order QCD calculations give a good description of the measurements, except for jets with low  $E_T^{\text{jet}}$  and high  $\eta^{\text{jet}}$ . The cross sections have the potential to improve the determination of the PDFs in future QCD fits. Values of  $\alpha_s(M_Z)$  have been extracted from the measurements based on different jet algorithms. In addition, the energy-scale dependence of the strong coupling was determined.

*The European Physical Society Conference on High Energy Physics  
18-24 July 2013  
Stockholm, Sweden*

---

<sup>\*</sup>Speaker.

<sup>†</sup>On behalf of the ZEUS collaboration.

## 1. Introduction

The measurement of jet photoproduction (PHP) at HERA provides a high-statistics test of perturbative QCD (pQCD) in a process with a single hard scale,  $E_T^{\text{jet}}$ . Jet cross sections allow precise determinations of the strong coupling constant,  $\alpha_s$ , and its energy dependence.

At leading order, so-called direct and resolved processes contribute to jet photoproduction. In direct processes, the photon interacts directly with a parton in the proton. On the other hand, the photon acts as a source of partons for the resolved contributions. Hence inclusive-jet cross sections are directly sensitive to the proton and photon PDFs.

The  $k_T$  cluster algorithm [1] in the longitudinally invariant inclusive mode [2] results in small theoretical uncertainties and hadronisation corrections in electron-proton collisions. It yields infrared- and collinear-safe cross sections at any order of QCD. More recently, new infrared- and collinear-safe algorithms like anti- $k_T$  [3] or SIScone [4] were developed. Jet photoproduction at HERA represents a well-understood hadron-induced reaction to test and compare the performances of these different jet clustering algorithms.

NLO QCD predictions [5] are compared to the measured inclusive-jet cross sections. The renormalisation and factorisation scales were set to  $\mu_R = \mu_F = E_T^{\text{jet}}$  and the number of flavours was chosen to be five. Unless explicitly stated otherwise, the ZEUS-S [6] parametrisations were used for the proton PDFs and the GRV-HO [7] sets were chosen for the photon PDFs. Hadronisation corrections were obtained using the `Pythia` [8] and `Herwig` [9] Monte Carlo (MC) programs. For comparisons, samples of `Pythia` including multi-parton interactions [10], `Pythia-MI`, were used to estimate the contribution from non-perturbative effects not related to hadronisation. For all three jet algorithms introduced above, missing terms beyond NLO represent the dominant uncertainty of the predictions.

## 2. Differential inclusive-jet cross sections

Single- and double-differential inclusive-jet cross sections have been measured in the reaction  $ep \rightarrow e + \text{jet} + X$  for  $142 < W_{\gamma p} < 293$  GeV, where  $W_{\gamma p}$  is the  $\gamma p$  centre-of-mass energy, and  $Q^2 < 1$  GeV<sup>2</sup> with the ZEUS detector at HERA using an integrated luminosity of 300 pb<sup>-1</sup>. The cross sections include every jet with  $E_T^{\text{jet}} > 17$  GeV and  $-1 < \eta^{\text{jet}} < 2.5$  [11].

Single-differential cross sections based on the  $k_T$  algorithm as functions of  $E_T^{\text{jet}}$  and  $\eta^{\text{jet}}$  are shown in Fig. 1. The uncertainty on the jet energy scale of  $\pm 1\%$  typically leads to a  $\mp 5\%$  uncertainty on the measured cross sections which is fully correlated between measurements in different bins. At high  $E_T^{\text{jet}}$  this uncertainty increases to  $\mp 10\%$ . The measurements are well described by NLO QCD except for  $\eta^{\text{jet}} > 2$ . The disagreement in the forward region disappears if the kinematic region of the measurement is restricted to  $E_T^{\text{jet}} > 21$  GeV.

Alternative NLO QCD predictions based on the HERAPDF1.5 [12] and MSTW08 [13] proton PDFs instead of ZEUS-S are also shown in Fig. 1. The predictions based on HERAPDF1.5 are lower than those based on ZEUS-S in most of the investigated phase-space region. Especially at large  $E_T^{\text{jet}}$ , the usage of MSTW08 instead of ZEUS-S in the NLO QCD calculations leads to higher predictions. The high-precision measurements of inclusive-jet photoproduction have the potential to constrain the proton PDFs in future QCD fits.

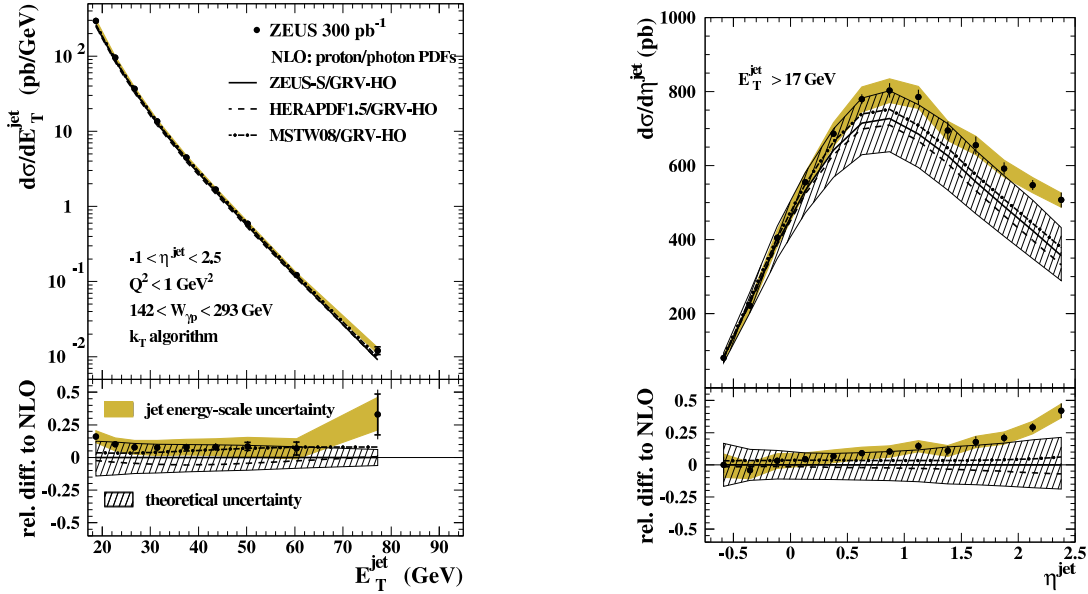


**Figure 1:** Single-differential cross sections  $d\sigma/dE_T^{\text{jet}}$  (left) and  $d\sigma/d\eta^{\text{jet}}$  (right) based on the  $k_T$  algorithm. The data are compared to NLO QCD predictions based on different proton PDFs.

In addition, inclusive-jet cross sections based on the  $k_T$  algorithm were determined as functions of  $E_T^{\text{jet}}$  in different regions of  $\eta^{\text{jet}}$ . As observed for the single differential cross sections, the data are well described by NLO QCD except at  $E_T^{\text{jet}} < 21$  GeV for  $\eta^{\text{jet}} > 2$ .

### 3. Impact of multi-parton interactions

The effect of multi-parton interactions is not included in the NLO QCD calculations described in Sec. 1. Instead, correction factors were obtained using `Pythia-MI` including multi-parton interactions with a minimum transverse momentum of the secondary scatter,  $p_{T,\text{min}}^{\text{sec}}$ , of 1, 1.5 and 2 GeV. Single-differential cross sections based on the  $k_T$  algorithm as functions of  $E_T^{\text{jet}}$  and  $\eta^{\text{jet}}$  are compared to NLO QCD predictions where these correction factors have been applied are shown in Fig. 2. The inclusion of multi-parton interactions increase the predictions at low  $E_T^{\text{jet}}$  and large  $\eta^{\text{jet}}$ . The best description of the data is observed for  $p_{T,\text{min}}^{\text{sec}} = 1.5$  GeV.

### 4. Comparison of different jet algorithms

Differential cross sections for inclusive-jet photoproduction as functions of  $E_T^{\text{jet}}$  and  $\eta^{\text{jet}}$  were measured for the  $k_T$ , anti- $k_T$  and SIScone jet algorithms. The hadronisation corrections are largest for the SIScone algorithm while similar corrections were found for the  $k_T$  and anti- $k_T$  algorithms. As shown for the  $k_T$  algorithm above, the measurements based on anti- $k_T$  and SIScone are well described by NLO QCD except at large  $\eta^{\text{jet}}$ .

To compare the different jet algorithms in detail, the ratios of the measured cross sections anti- $k_T/k_T$ , SIScone/ $k_T$  and anti- $k_T$ /SIScone were determined and are shown in Fig. 3. The cross

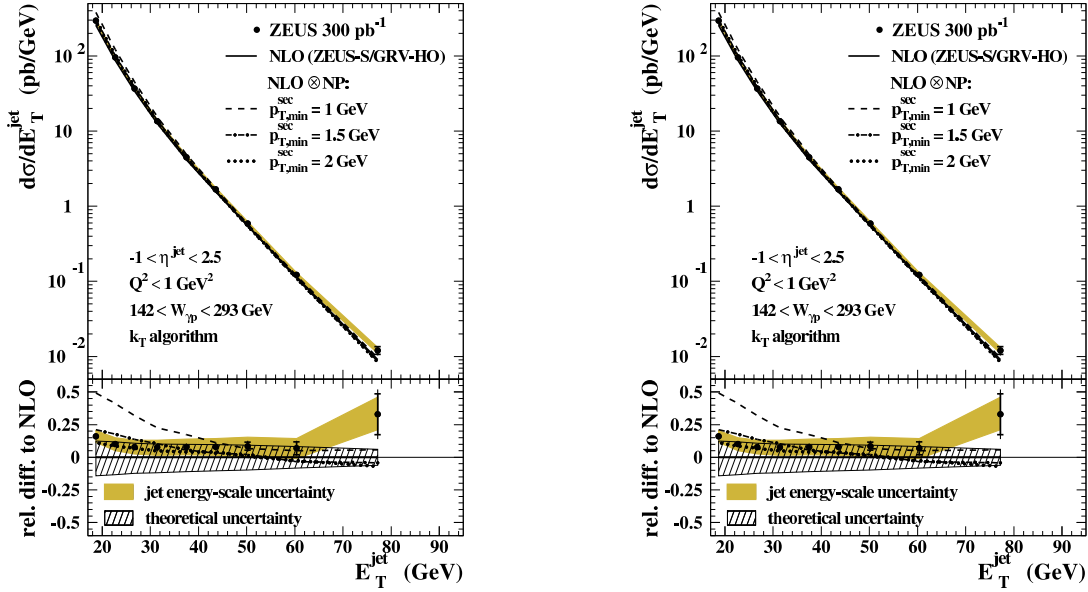


**Figure 2:** Single-differential cross sections  $d\sigma/dE_T^{\text{jet}}$  (left) and  $d\sigma/d\eta^{\text{jet}}$  (right) based on the  $k_T$  algorithm. The data are compared to NLO QCD predictions. For comparison, the NLO QCD calculations including an estimation of non-perturbative effects are shown in addition.

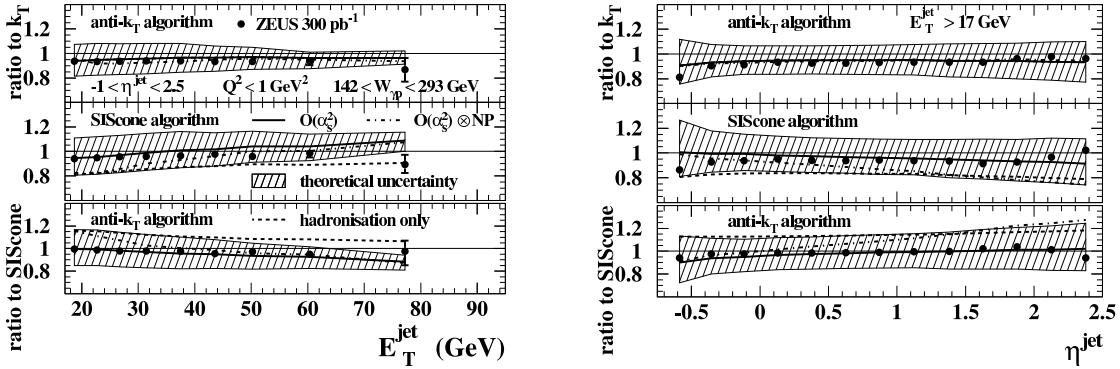


**Figure 3:** The ratios of the measured cross sections  $\text{anti-}k_T/k_T$ ,  $\text{SIScone}/k_T$  and  $\text{anti-}k_T/\text{SIScone}$  as functions of  $E_T^{\text{jet}}$  (left) and  $\eta^{\text{jet}}$  (right).

sections for  $\text{anti-}k_T$  have the same shape as those for  $k_T$ , but are about 6% smaller. The measured cross sections based on SIScone have a slightly different shape than those based on  $k_T$  or  $\text{anti-}k_T$ . The QCD calculations with up to three partons in the final state describe the measured ratios.

## 5. Determination of $\alpha_s$ and its energy-scale dependence

The measured single-differential cross sections  $d\sigma/dE_T^{\text{jet}}$  for  $21 < E_T^{\text{jet}} < 71$  GeV based on the  $k_T$ ,  $\text{anti-}k_T$  and SIScone jet algorithms were used to determine  $\alpha_s(M_Z)$  [14]. Consistent results were obtained for all three jet algorithms:

$$\begin{aligned}\alpha_s(M_Z)|_{k_T} &= 0.1206^{+0.0023}_{-0.0022} \text{ (exp.) } ^{+0.0042}_{-0.0035} \text{ (th.)}, \\ \alpha_s(M_Z)|_{\text{anti-}k_T} &= 0.1198^{+0.0023}_{-0.0022} \text{ (exp.) } ^{+0.0041}_{-0.0034} \text{ (th.)}, \\ \alpha_s(M_Z)|_{\text{SIScone}} &= 0.1196^{+0.0022}_{-0.0021} \text{ (exp.) } ^{+0.0046}_{-0.0043} \text{ (th.)}.\end{aligned}$$

The results are in agreement with other determinations of  $\alpha_s(M_Z)$  [11]. In addition, values of  $\alpha_s$  were extracted at the mean values,  $\langle E_T^{\text{jet}} \rangle$ , of the bins in  $E_T^{\text{jet}}$  without assuming the running of  $\alpha_s$ . The extracted values of  $\alpha_s$  as a function of  $E_T^{\text{jet}}$  are shown in Fig. 4. This measurement confirms the running of  $\alpha_s$  over a wide  $E_T^{\text{jet}}$  range. The observed running is in good agreement with the two-loop QCD prediction.

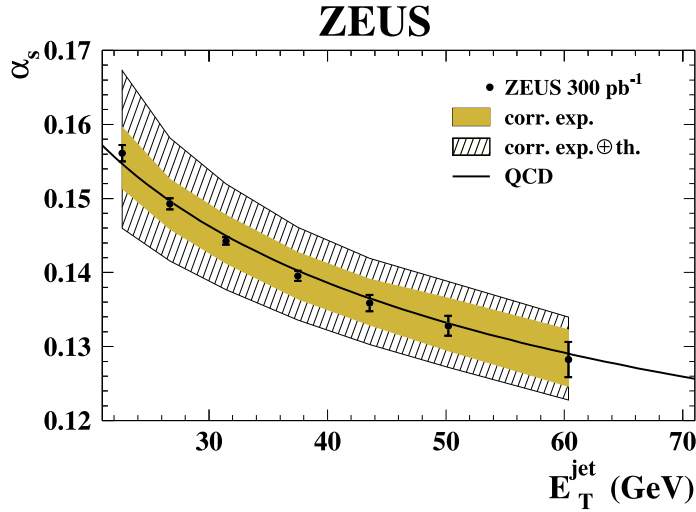


**Figure 4:**  $\alpha_s$  extracted at various  $\langle E_T^{\text{jet}} \rangle$  values from the measured  $d\sigma/dE_T^{\text{jet}}$  cross sections based on the  $k_T$  algorithm.

## 6. Summary and conclusions

Inclusive-jet cross sections in photoproduction were measured using the ZEUS detector. The data are generally well described by NLO QCD predictions. The inclusion of multi-parton interactions improves the predictions at low  $E_T^{\text{jet}}$  and large  $\eta^{\text{jet}}$ . The presented measurements have the potential to improve the photon and proton PDFs in future QCD fits. The strong coupling constant was extracted at the  $Z$  mass with competitive precision compared to other measurements and over a wide  $E_T^{\text{jet}}$  range.

## References

- [1] S. Catani et al., *Longitudinally-invariant  $k_{\perp}$ -clustering algorithms for hadron-hadron collisions*, Nucl. Phys. **B 406**, 187 (1993).
- [2] S.D. Ellis and D.E. Soper, *Successive combination jet algorithm for hadron collisions*, Phys. Rev. **D 48**, 3160 (1993).

- [3] M. Cacciari, G.P. Salam and G. Soyez, *The anti- $k_t$  jet clustering algorithm*, JHEP **04**, 063 (2008).
- [4] G.P. Salam and G. Soyez, *A practical seedless infrared-safe cone jet algorithm*, JHEP **05**, 086 (2007).
- [5] M. Klasen, T. Kleinwort and G. Kramer, *Inclusive jet production in  $\gamma p$  and  $\gamma\gamma$  processes: direct and resolved photon cross sections in next-to-leading order QCD*, Eur. Phys. J. C **1**, 1 (1998).
- [6] S. Chekanov et al., *ZEUS next-to-leading-order QCD analysis of data on deep inelastic scattering*, Phys. Rev. D **67**, 012007 (2003).
- [7] M. Glück, E. Reya, A. Vogt, *Parton structure of the photon beyond the leading order*, Phys. Rev. D **45**, 3986 (1992);  
M. Glück, E. Reya, A. Vogt, *Photonic parton distributions*, Phys. Rev. D **46**, 1973 (1992).
- [8] T. Sjöstrand, *High-energy-physics event generation with PYTHIA 5.7 and JETSET 7.4*, Comput. Phys. Comm. **82**, 74 (1994).
- [9] G. Marchesini et al., *HERWIG 5.1 - a Monte Carlo event generator for simulating hadron emission reactions with interfering gluons*, Comput. Phys. Comm. **67**, 465 (1992);  
G. Corcella et al., *HERWIG 6: an event generator for hadron emission reactions with interfering gluons (including supersymmetric processes)*, JHEP **01**, 010 (2001).
- [10] T. Sjöstrand and M. van Zijl, *A multiple-interaction model for the event structure in hadron collisions*, Phys. Rev. D **36**, 2019 (1987).
- [11] H. Abramowicz et al., *Inclusive-jet photoproduction at HERA and determination of  $\alpha_s$* , Nucl. Phys. B **864**, 1 (2012) [[arXiv:1205.6153](#)].
- [12] F.D. Aaron, *Combined measurement and QCD analysis of the inclusive  $e^\pm$  scattering cross sections at HERA*, JHEP **01**, 109 (2010).
- [13] A.D. Martin et al., *Parton distributions for the LHC*, Eur. Phys. J. C **63**, 189 (2009).
- [14] S. Chekanov et al., *Inclusive jet cross sections in the Breit frame in neutral current deep inelastic scattering at HERA and determination of  $\alpha_s$* , Phys. Lett. B **547**, 164 (2002).